CaATP as a Substrate to Investigate the Myosin Lever Arm Hypothesis of Force Generation

Katherine Polosukhina,* Don Eden,† Marc Chinn,‡ and Stefan Highsmith*

*Department of Biochemistry, University of the Pacific, School of Dentistry, San Francisco, California 94115-2399; †Department of Chemistry and Biochemistry, San Francisco State University, San Francisco, California 94132; and ‡Cardiovascular Research Institute, University of California, San Francisco, California 94143 USA

ABSTRACT In an effort to test the lever arm model of force generation, the effects of replacing magnesium with calcium as the ATP-chelated divalent cation were determined for several myosin and actomyosin reactions. The isometric force produced by glycerinated muscle fibers when CaATP is the substrate is 20% of the value obtained with MgATP. For myosin subfragment 1 (S1), the degree of lever arm rotation, determined using transient electric birefringence to measure rates of rotational Brownian motion in solution, is not significantly changed when calcium replaces magnesium in an S1-ADP-vanadate complex. Actin activates S1 CaATPase activity, although less than it does MgATPase activity. The increase in actin affinity when S1 · CaADP · P_i is converted to S1 · CaADP is somewhat greater than it is for the magnesium case. The ionic strength dependence of actin binding indicates that the change in apparent electrostatic charge at the acto-S1 interface for the S1 · CaADP · P_i to S1 · CaADP step is similar to the change when magnesium is bound. In general, CaATP is an inferior substrate compared to MgATP, but all the data are consistent with force production by a lever arm mechanism for both substrates. Possible reasons for the reduced magnitude of force when CaATP is the substrate are discussed.

INTRODUCTION

The actin-based molecular motor myosin generates force by coupling mechanical action to binding and hydrolysis of a substrate. The natural substrate is MgATP. In muscle, an actin filament is surrounded by an array of myosin motor domains. Force impulses to actin are coupled to cycles of ATP hydrolysis by the motor domains. The mechanical action of each cycle is currently hypothesized to involve rotation of a segment of the motor domain, called the lever arm. According to the lever arm hypothesis, MgATP binding dissociates a motor domain from actin. A hydrolysis-coupled rotation of the lever arm then occurs while myosin is free, and force is produced by reversal of the rotation after the motor domain rebinds to actin. Associated with the reverse rotation, the hydrolysis products dissociate and the motor domain affinity for actin increases. For more detail, muscle contraction (Cooke, 1997) and the lever arm model of force generation (Geeves and Holmes, 1999; Highsmith, 1999) have been reviewed recently. Although the lever arm mechanism has yet to be proven, several kinetic and structural features of the model can be quantitatively assessed. One approach to testing the validity of the model is to compare these features for MgATP and a non-natural substrate.

Here we examine CaATP as a substrate for skeletal muscle fibers and for isolated myosin motor domain (subfragment 1 or S1) and actin. CaATP has been suggested to be a poor or non-force-generating substrate for muscle fibers (Szent-Gyorgyi, 1947), although to the best of our knowledge no fiber data have been published. Some data exist for model systems. The force that is produced by contraction of actomyosin threads is lower for CaATP than for MgATP (Bowen, 1952). The degree of superprecipitation is reduced when CaATP is the substrate (Weber and Portzehl, 1954). We measured isometric force production by glycerinated muscle fibers in the presence of CaATP and confirm that it is lower than observed for MgATP under the same conditions. In addition, several structural, energetic, and kinetic features of the CaATP-myosin-actin system in solution were determined and compared to the MgATP case. Conditions as close as possible to those of the force measurements were used. The steady-state kinetic parameters for basal and actin-activated CaATPase activities of S1 were measured. The degree of lever arm rotation of S1 · CaADP · V_i, S1 · CaADP, and S1 · Ca in solution were compared to their magnesium counterparts by using transient electric birefringence (TEB). The actin affinity and apparent electrical charge at the interface were measured for S1 · CaADP · P_i and S1 · CaADP. Our goals are to test the lever arm hypothesis and to use the model to understand what elements of the hydrolytic and/or mechanical cycles may be responsible for the differences in force generation by CaATP and MgATP.

MATERIALS AND METHODS

Fiber, protein, and buffer preparation

Fibers were obtained from strips of rabbit psoas muscle, which were dissected and stored in 50% glycerol, 50 mM Mops, 120 mM KOAc, 5 mM $MgCl_2$, 1 mM EGTA, pH 7 at 0°C for 24 h and then at −20°C for several weeks before use (Cooke and Pate, 1985). Myosin was isolated from rabbit skeletal muscle (Nauss et al., 1969) and S1 with both light chains present was produced from myosin by proteolysis using papain (Margossian and

Received for publication 2 August 1999 and in final form 14 December 1999.

Address reprint requests to Stefan Highsmith, Department of Biochemistry, University of the Pacific, San Francisco, CA 94115-2399. Tel.: 415-929-6670; Fax: 415-929-6654; E-mail: shighsmith@uop.edu.

0006-3495/00/03/1474/08 $2.00

Lowey, 1982) and purified by ion exchange and size exclusion chromatography (Weeds and Taylor, 1975; Highsmith, 1997). Actin was isolated from rabbit skeletal muscle (Spudich and Watt, 1971), dialyzed against a specific buffer, pelleted by centrifugation, and resuspended in the buffer for use. Buffers were made using reagent-grade chemicals and glass-distilled water additionally deionized to greater than 18.0×10^6 Ohm-cm resistivity using a Barnstead water purification system. Contaminating $[Mg^{2+}]$ in the calcium buffers was measured by an induction-coupled plasma method (QTI, Whitehouse, NJ).

Force measurement

Individual fibers were dissected from a glycerinated psoas muscle preparation and attached to a force transducer (Pate et al., 1993). Fiber length and diameter were measured (Cooke and Pate, 1985). The measured force was normalized for fiber cross-section and is reported in mN/mm^2. As a control for a glycerinated muscle fiber preparation, the force for an individual fiber was measured at 10°C in 50 mM Mops (pH 7.0), 120 mM KOAc, 5 mM $MgCl_2$, 1 mM EGTA, 1.10 mM $CaCl_2$, 20 mM creatine phosphate, 1 mg/ml creatine phosphokinase, 4 mM ATP, and 3 mM K_3PO_4. Only glycerinated muscle preparations with fibers producing force consistent with published values (Pate et al., 1993) were used as a source of individual fibers for the calcium measurements.

To measure force generation from CaATP hydrolysis, a fiber was mounted and incubated in 20 mM Mops, 1 mM EDTA, pH 7 for 10 min. This wash to remove endogenous Mg^{2+} was repeated at least twice, and in some cases was lengthened to 20 min. The buffer was changed to 20 mM Mops (pH 7.0), 4 mM $CaCl_2$, and contraction was initiated by adding ATP to obtain 3 mM. This buffer and the ones used in the other experiments described below were chosen to obtain conditions as near as possible to identical in all cases. The ionic strength is low to optimize the TEB measurements. The divalent cation concentration is high to ensure saturation of the ATP binding site by the various metal ion-nucleotide complexes.

S1 ATPase activities

The steady-state rates of CaATP and MgATP hydrolyses by S1 were measured at 25°C in 10 mM Mops (pH 7.0), 2 mM ATP plus either 5 mM $CaCl_2$ or 5 mM $MgCl_2$, respectively. Aliquots were taken at increasing times after the reaction was initiated, and [phosphate] was detected by a Malachite green method (Kodama et al., 1986). S1 was 1.0–1.5 μM for MgATPase and 0.50–0.80 μM for CaATPase activity measurements. Actin-activated activities were measured with 2–60 μM F-actin in the same buffers.

S1-phosphate analog complex stabilities

The rates of formation of complexes of S1, ADP, orthovanadate, and either Ca^{2+} or Mg^{2+} were determined at 25°C by measuring the loss of ATPase activity. Conditions similar to those of Goodno (1979) for inactivation of S1 by vanadate in the presence of Mg^{2+} were modified to obtain low ionic strength samples suitable for TEB measurements (Highsmith and Eden, 1990), and used for both Ca^{2+} or Mg^{2+}. S1 (10 μM) was incubated in 10 mM Mops (pH 7.0), 0.20 mM ADP, and 5 mM $CaCl_2$ or 5 mM $MgCl_2$ for 10 min. A stock solution of orthovanadate (Goodno, 1979) was used to obtain 0.50 mM vanadate to start the reaction. At increasing times aliquots were taken and diluted to obtain 1 μM S1 in 10 mM Mops (pH 7.0), 2 mM ATP, and either 5 mM $CaCl_2$ and 5 mM $MgCl_2$. The ATPase activity was determined from the rate of phosphate production, measured using Malachite green.

The rates of dissociation of orthovanadate from the inactive complexes were determined by measuring the increase of KATPase activity in the presence of EDTA. 10.0 μM S1 complexes in 10 mM Mops (pH 7.0), 0.20 mM ADP, either 5 mM $CaCl_2$ or 5 mM $MgCl_2$, and 0.50 mM sodium orthovanadate were incubated 16 h at 0°C to achieve maximal inactivation. A solution of inactive S1 was warmed quickly to 25°C and diluted with 20 mM EDTA to obtain 5.0 μM S1 complex and 10 mM EDTA. Aliquots were taken at increasing times and diluted to give 0.50 μM S1 in 50 mM Tris (pH 8.0), 600 mM KCl, 2.0 mM ATP, 6.0 mM EDTA. Phosphate production was determined using Malachite green.

S1 hydrodynamic size changes

The rates of rotational Brownian diffusion of S1 and S1-nucleotide complexes in 10 mM Mops (pH 7.0) and either 5.0 mM $CaCl_2$ or 5.0 mM $MgCl_2$ were determined at 3.7°C. The S1 permanent electric dipole was partially aligned by a 10-μs 3570 V/cm electric field pulse. The decay of the birefringence signal after the electric field was removed was analyzed using the program DISCRETE (Provencher, 1976) to determine the rotational decay time(s), τ_i. The decay data were always best fitted by a single exponential decay function. The instrumentation has been described (Elias and Eden, 1981; Eden and Highsmith, 1997). The rate of rotational Brownian diffusion is related to hydrodynamic size. Low-resolution structures of S1, obtained from fits of the rotational decay data using models of S1 that are bent to various degrees about a hinge at its center (Highsmith and Eden, 1990), are in quantitative agreement with high-resolution S1 atomic structures (Rayment et al., 1993).

S1 actin binding

The association constants at 25°C for actin binding to the complexes S1 · MeADP and S1 · MeADP · P_i, where Me is either magnesium or calcium, were measured using a cosedimentation method (Highsmith and Murphy, 1992) in the same buffers used for the force measurements. The steady-state intermediates S1 · MgADP · P_i and S1 · CaADP · P_i were maintained by excess ATP in the solution.

Acto-S1 interface electrostatic charge

The product of the net effective electrostatic charge on the actin and myosin sides of the binding interface, $z_M z_A$, was estimated for binding in solution. Actin binding to S1 · MeADP and S1 · MeADP · P_i, where Me is either magnesium or calcium, was measured in solutions of increasing ionic strength and $z_M z_A$ was calculated by the method of Pitzer (Pitzer, 1979; Highsmith and Murphy, 1992).

RESULTS

Force production

At 10°C in 27 mM ionic strength buffer, isometric force is produced by glycerinated skeletal muscle fibers when CaATP is the substrate (Fig. 1). The steady-state force, in the plateau following the rapid initial rise, is 54 ± 15 mN/mm^2 ($n = 5$), compared to 289 ± 84 mN/mm^2 ($n = 5$) observed when Mg^{2+} is substituted for Ca^{2+} (data not shown). Because of the low ionic strength of the buffer, the peak force produced in the presence of MgATP is somewhat higher than observed by others under more physiological conditions (Pate et al., 1993). This is the first report of force production by a muscle fiber due to CaATP hydrolysis. The low ionic strength buffer was chosen to maximize interac-

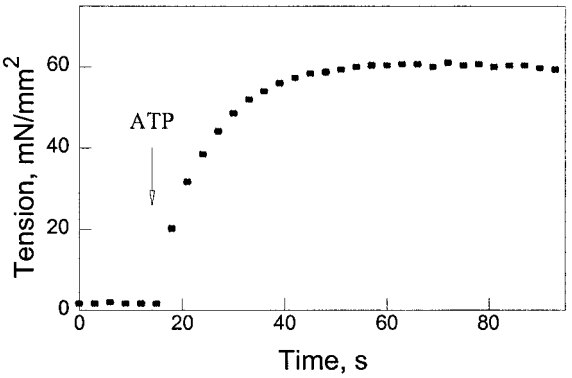

FIGURE 1 Isometric force production. A glycerinated muscle fiber at 10°C was bathed in an EDTA buffer for several changes and then transferred to a Ca^{2+} buffer, as described in Materials and Methods. When ATP was added, tension increased smoothly to 54 ± 15 mN/mm^2.

tions between actin and myosin in the fibers. However, if after 120 s KCl was added to the bath to obtain 10, 50, and 100 mM KCl, it had a negligible effect on the force produced in the presence of calcium (data not shown).

A potential problem is that the force observed when ATP is added to a fiber bathed in the Ca^{2+} buffer might be due to the hydrolysis of MgATP formed from Mg^{2+} contamination, either from the fiber or from the buffers. To test the fiber as a source of Mg^{2+}, we varied the number and duration of EDTA washes that were done before it was immersed in the Ca^{2+} buffer and force was measured (see Materials and Methods). The force produced was unchanged within the experimental error after one to three 10-min washes, or one 20-min wash. These control measurements indicate that the fiber is not a significant source of Mg^{2+} in the procedure used. The Ca^{2+} and ATP buffers were also analyzed for Mg^{2+}. One method was to tabulate the trace amounts of Mg^{2+} in the reagents and water used to prepare the buffers, using manufacturer specifications. By this method the total [Mg^{2+}] was <2.1 μM. Contaminating [Mg^{2+}] in the Ca^{2+} buffer was also measured, by induction coupled plasma analysis. Total [Mg^{2+}] was below the detection limit, <5 μM. When 5 μM $MgCl_2$ was added to a fiber contracting in the Ca^{2+} buffer, the force increased by $<2\%$. It appears that the force observed for glycerinated muscle fibers, 20% of that obtained with MgATP, is due to the binding and hydrolysis of CaATP.

Lever arm rotation

Rotation of the S1 lever arm to form a more compact motor domain structure was measured using TEB (Highsmith and Eden, 1990). Using a weak electric field to partially align an S1 complex, the rotational decay time, τ, was measured for the rotation back to random orientation after the electric field was removed. The smaller τ is, the more compact is the structure of the complex. Measurements were made for 1.0 μM S1, S1 · CaADP, and S1 · CaADP · V_i (Table 1). Parallel measurements were made with $MgCl_2$ replacing $CaCl_2$. The vanadate complexes were prepared at 0°C and incubated overnight before making the transient electric birefringence measurements. The MgATPase and CaATPase activities were 8% and 14% of normal, respectively, confirming that the complexes were formed.

The data (Table 1) indicate that comparable changes in hydrodynamic size are induced by ligand binding for the calcium and magnesium complexes. The most important observation is that the decrease in τ for S1 · CaADP · V_i, compared to S1 · CaADP, is quantitatively close to the decrease observed for S1 · MgADP · V_i, compared to S1 · MgADP. Assuming that in both cases decreases in τ are due to lever arm rotation, the ratio of $\tau_{ADP\,.\,Vi}/\tau_{ADP}$ is a quantitative indicator of the degree of rotation. The ratio is 0.92 for the calcium complexes and 0.94 for the magnesium complexes. S1 · MgADP · V_i is considered to be a analog of S1 · MgADP · P_i (Goodno, 1979), although it is not clear as to whether it best represents a transition state or hydrolysis products (Smith and Rayment, 1996a; Ajtai et al., 1998). The magnesium complex has the lever arm rotated (Highsmith and Eden, 1990). The data for ADP and ADP · V_i strongly suggest that similar degrees of lever arm rotation occur for magnesium and calcium complexes when ATP is hydrolyzed.

The rotational times for the calcium complexes are smaller in all cases than for the magnesium analogs. This is true even in the absence of nucleotide, suggesting that Ca^{2+} is binding to S1 independently of binding as a nucleotide-complex. The effect on τ of nucleotide-independent Ca^{2+} binding appears to be additive to the effect of nucleotide-dependent binding.

S1 · CaADP · V_i stability

The observed loss of S1 activity in the presence of Mg^{2+} or Ca^{2+} plus ADP and orthovanadate indicates that the complexes prepared for TEB measurements are stable in the buffer used for those measurements. To quantitatively assess the relative stabilities of the S1 · MgADP · V_i and S1 · CaADP · V_i complexes, the rates of complex formation and dissociation were measured. The loss of CaATPase activity after the addition of V_i to S1 · CaADP is shown in Fig. 2 *A*.

TABLE 1 Myosin S1 rotational decay times

Ligand	τ_{Mg2+} (ns)	τ_{Ca2+} (ns)
None	421.6 ± 2.4	417.4 ± 1.3
ADP	428.3 ± 1.1	413.8 ± 1.7
ADP · V_i	396.2 ± 2.2	383.8 ± 2.4

The rates of rotational Brownian motion at 3.7°C were determined by TEB, as described under Materials and Methods. Solutions contained 1μM S1, 10 mM Mops, with either 5 mM $CaCl_2$ or 5 mM $MgCl_2$, and ligands as indicated at 0.20 mM ADP, 0.50 mM V.

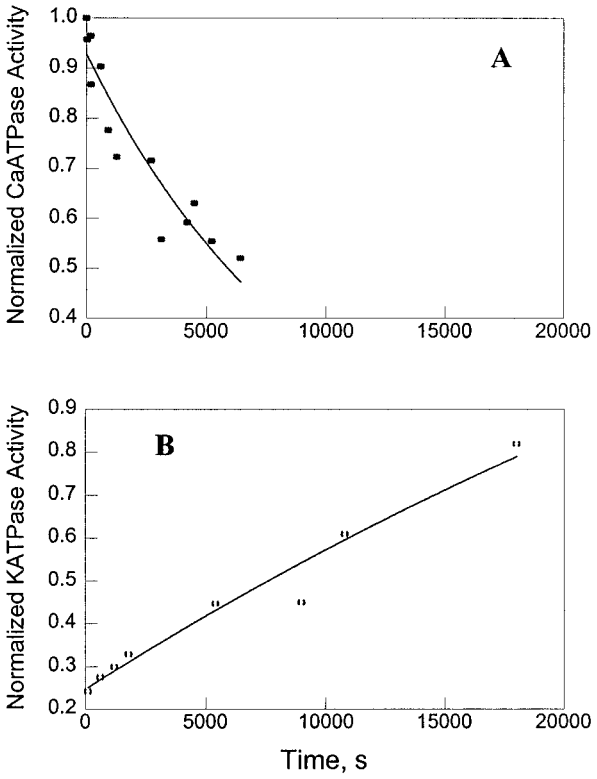

FIGURE 2 Formation and dissociation of S1 · CaADP · V_i. (*A*) Orthovanadate was added to S1 · CaADP at 25°C and the loss of CaATPase activity (*filled circles*) was measured for aliquots taken at increasing times, as described in Materials and Methods. The rate was determined for the exponential loss of activity. When Mg^{2+} was substituted for Ca^{2+} (data not shown), the rate was much faster (Table 2). (*B*) EDTA was added to a solution of the inactive complex at 25°C and the increase of KATPase activity (*open circles*) was measured for aliquots taken at increasing times. The data were fitted by a single exponential function to determine the rate. When Mg^{2+} was substituted for Ca^{2+}, the rate was similar (Table 2).

A pseudo-first-order rate constant, k_1, determined by fitting the data with the equation

$$A = A_o\exp(-k_1 t),$$

is 1.1×10^{-4} s^{-1}, where A and A_o are the activities in the presence and absence of orthovanadate, respectively. The rate of dissociation V_i from the complex was measured in the presence of EDTA. EDTA scavenges Ca^{2+}, and it is assumed that the dissociation rates of CaADP from S1 · CaADP and of Ca^{2+} from CaADP are much faster than the dissociation rate of V_i from S1 · CaADP · V_i. The increase in KATPase activity after the addition of EDTA to the inactivated complex is shown in Fig. 2 *B*. When the data are fitted using the equation

$$A = A_o[1 - \exp(-k_1 t)],$$

k_{-1} is 2.0×10^{-5} s^{-1}. When Mg^{2+} is substituted for Ca^{2+}, k_{-1} is little changed, but k_1 is much larger (Table 2). The Ca^{2+} complex is the less stable of the two, consistent with the calcium complex being too unstable to detect under some conditions (Peyser et al., 1996).

TABLE 2 Rates of S1 · CaADP · V_i and S1 · MgADP · V_i formation and dissociation

	Calcium	Magnesium
Formation, s^{-1}	$(1.1 \pm 0.1) \times 10^{-4}$	$(1.7 \pm 0.4) \times 10^{-2}$
Dissociation, s^{-1}	$(2.0 \pm 0.9) \times 10^{-5}$	$(3.1 \pm 1.9) \times 10^{-5}$

For the pseudo-first-order rates of formation, orthovanadate was added to start the reaction (see Materials and Methods for reaction conditions). Aliquots were taken and the ATPase activity was determined (Fig. 2). The loss of activity was fitted using a single exponential decay function. For dissociation rates, the inactivated complex was incubated in the presence of EDTA, aliquots were taken, and KATPase activity was determined.

Actin activation of S1 CaATPase activity

To compare the mechanisms of force production from the hydrolysis of CaATP to that from MgATP, it is important to determine whether actin interacts with the steady-state intermediate S1 · CaADP · P_i and accelerates the rate of product dissociation. The basal CaATPase activity in the absence of actin is high, approaching that of actin-activated MgATPase activity. At 25°C in the buffer used for the fiber force measurements, S1 CaATPase activity is 1.6 s^{-1}, consistent with published values (Shriver and Sykes, 1981; Wagner and Giniger, 1981). This is 40-fold higher than S1 MgATPase activity for the same conditions (Table 3). Actin activates the rate of CaATP turnover, but only 2.4-fold when the data for the lower [actin] range are fitted assuming Michaelis-Menten kinetics (Fig. 3). There is 90-fold activation for MgATP hydrolysis for the same conditions (Table 3). The reduced actin-activation when calcium is present is due at least partially to the high basal CaATPase activity. Actin activation of CaATPase activity is sensitive to conditions, and has been reported to be as low as 1.5-fold (Nihei and Tonomura, 1959) and as high as 22-fold (Peyser et al., 1996). The apparent K_m for actin activation is 20-fold higher for CaATPase than it is for MgATPase activity (Table 3). The higher K_m and reduced activation indicate

TABLE 3 Steady-state ATPase activities

	Calcium	Magnesium
S1 ATPase, s^{-1}	1.64 ± 0.12	0.045 ± 0.007
Actin-activated S1 ATPase V_{max}, s^{-1}	3.8 ± 0.7	4.1 ± 0.7
K_m, μM	50 ± 26	2.5 ± 0.5

The steady-state rates were measured at 25°C in 10 mM Mops (pH 7.0), 4 mM ATP, and 5 mM $CaCl_2$. Aliquots were taken at increasing times after the reaction was initiated, and phosphate concentration was detected as described in Materials and Methods. V_{max} and K_m were determined by fitting the dependence of the activity on actin concentration up to 40 μM (Fig. 3), assuming Michaelis-Menten kinetics. The decrease in activity at higher actin concentration may be making the values obtained for V_{max} and K_m lower than the true values (see Discussion). Magnesium data are from Highsmith (1997).

that actin interaction with S1 · CaADP · P_i is less effective than it is with S1 · MgADP · P_i, but the data show that actin does bind to S1 · CaADP · P_i and accelerates the rate of product dissociation.

The decrease in CaATPase activity shown in Fig. 3 for [actin] above 40 μM was consistently observed. For technical reasons it was difficult to obtain data for [actin] $>$ 60 μM, so the CaATPase activity at saturating levels of actin was not determined. The decrease at higher [actin] may have introduced a systematic error of unknown magnitude into the results obtained from fitting the data in the lower [actin] range. This systematic error, if it exists, does not change the conclusion that actin activates S1 CaATPase activity, but it would make the measured K_m larger than the true value and the measured V_{max} smaller than the true value (Table 3). A similar decrease in MgATPase activity is observed at high [actin] (White et al., 1997). At low [actin] the rate-determining step for the MgATP hydrolysis cycle is A + S1 · MgADP · P_i $\rightarrow$ A · S1 · MgADP · P_i (White and Taylor, 1976). At high [actin], actin remains bound when MgATP binds to A · M and the rate-determining step in the cycle changes to A · S1MgATP $\rightarrow$ A · S1MgADP · P_i (White et al., 1997). The data (Fig. 3) suggest that this change of rate-determining step also occurs for the CaATP hydrolysis cycle.

S1-actin interactions

If force production from CaATP hydrolysis follows the same steps as it does for MgATP, actin affinity should increase by several orders of magnitude when P_i is released. This is the case (Table 4). In 200 mM ionic strength solution, the fitted value of K_A for S1 · CaADP · P_i binding to actin is 2.0×10^3 M^{-1} and increases to 2.7×10^7 M^{-1} for S1 · CaADP. This corresponds to an increase in standard free energy change for actin binding of -5.6 kcal/mol when phosphate is released, which is larger than the -3.2 kcal/mol change for actin binding to S1 · MgADP · P_i and S1 · MgADP (Table 4). There is more than enough binding energy available from the actin · S1 · CaADP · P_i to S1 · CaADP transition to support force generation.

TABLE 4 Actin affinities and electrostatic charge at S1-actin binding interface

Complex	ln K_A (0 M)	ln K_A (0.2 M)	$z_M z_A$ (esu^2)
S1 · MgADP · Pi	11.2 ± 0.2	8.7 ± 0.2	−6.4 ± 0.7
S1 · CaADP · Pi	13.0 ± 0.8	7.6 ± 0.7	−12.2 ± 2.5
S1 · MgADP	15.4 ± 0.1	14.1 ± 0.2	−3.6 ± 0.2
S1 · CaADP	20.8 ± 0.7	17.1 ± 0.5	−9.7 ± 1.2

Measurements were made at 25°C using cosedimentation methods (see Materials and Methods). K_A is the association constant at the ionic strength specified. ln K_A (0 M) is the association constant at zero ionic strength, obtained by extrapolation, and $z_M z_A$ is the product of the electric charge at the actin-motor domain interface, which is determined from the ionic strength dependence of the binding (Pitzer, 1979; Highsmith and Murphy, 1992).

The ionic strength dependence of actin binding provides information about electrical interactions at the binding interface. When equilibrium binding to actin of S1 · CaADP and of the steady-state intermediate S1 · CaADP · P_i are measured in the presence of increasing [KOAc], the apparent affinity of S1 · CaADP · P_i is more dependent on ionic strength than its magnesium counterpart (Fig. 4). S1 · CaADP binding to actin is also more dependent on ionic

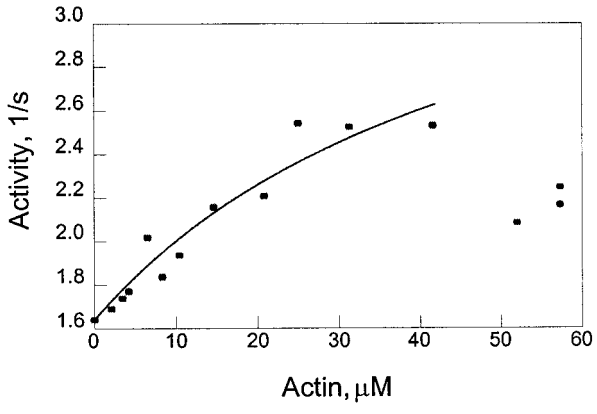

FIGURE 3 Actin activation of S1 CaATPase activity. F-actin was added to S1 at 25°C in the same buffer used for measuring tension by glycerinated fibers, and the activity was measured (see Materials and Methods). The data for [actin] up to 40 μM were fitted to the Michaelis-Menten equation to determine K_m and V_{max} (Table 3). At [actin] >40 mM the activity decreased, probably due to actin remaining bound to S1 · CaATP (see Discussion).

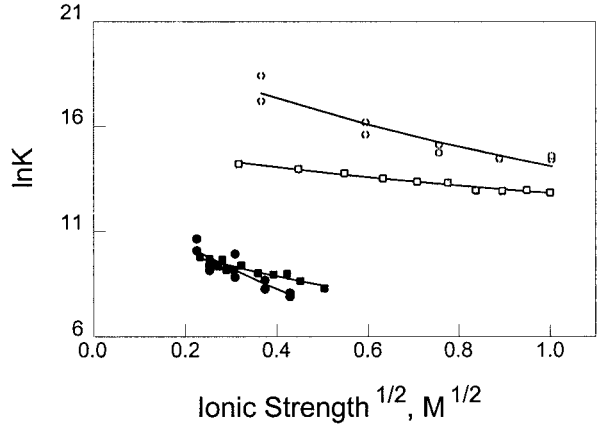

FIGURE 4 Ionic strength dependence of actin binding. Apparent association constants for actin binding to calcium and magnesium complexes were determined using a sedimentation method. The ionic strength dependence of actin binding to S1 · CaADP · P_i (*filled circles*) was greater that than to S1 · MgADP · P_i (*filled squares*), indicating there is more electrostatic charge at the actin-S1 · CaADP · P_i binding interface (see Table 4). Similarly, the ionic strength dependence of the actin affinity for S1 · CaADP (*open circles*) was greater than for S1 · MgADP (*open squares*). The magnitude of the actin affinity for S1 · CaADP was significantly larger than for S1 · MgADP at all ionic strengths.

strength than is that of S1 · MgADP. These data can be used to estimate the product of the net effective electric charge at the acto-S1 binding interface, $z_A z_M$ (Pitzer, 1979; Highsmith and Murphy, 1992). The calcium complexes have more apparent electrostatic charge at the acto-S1 interface than their magnesium counterparts (Table 4). In both cases the data indicate a decrease in apparent charge for the S1 · MeADP · P_i to S1 · MeADP transition (Table 4). The magnitude of the decrease is about the same (2.5 and 2.8 esu^2), despite the greater charge for the calcium complexes, suggesting that the structural changes at the actin binding site, which occur when P_i dissociates, are similar.

DISCUSSION

CaATP hydrolysis supports force production (Fig. 1). One goal is to determine whether the force production by CaATP is consistent with the lever arm model. According to that model, properties that are required for a substrate to support contraction include:

1. The substrate must be hydrolyzed by myosin;
2. Rotation of the lever arm must occur while the motor domain is dissociated from actin;
3. Actin must bind to the motor domain before the products dissociate and the lever arm returns to its original orientation;
4. The lever arm must change its orientation while the motor domain is bound to actin;
5. The actin affinity of the motor domain should increase as a result of product dissociation.

These properties describe a minimal contractile cycle, based on a simple kinetic scheme, which has the motor domain free from actin during part of the cycle (Lymn and Taylor, 1971). The real case is more complex, but the key elements of the lever arm model are explicit, making the above list useful for discussing the CaATP results.

The first property, that CaATP is a substrate for myosin and acto-myosin, is well established by measurements made as long ago as 40 years (Nihei and Tonomura, 1959). It is confirmed here for the buffer used in the fiber experiments (Table 3).

The TEB data provide strong evidence that the lever arm rotates when S1 · CaADP · V_i is formed (Table 1). The ratio of $\tau_{ADP \cdot Vi}/\tau_{ADP}$ is almost identical for the two cases, suggesting that S1 · CaADP · P_i has the lever arm rotated, and to a degree similar to that of S1 · MgADP · P_i. The second requirement in the above list is also satisfied.

It is interesting that in the absence of nucleotide, Ca^{2+} has an effect on the hydrodynamic size of S1. Ca^{2+} must be binding to S1 independently from the nucleotide-chelated mechanism (Table 1). The divalent cation binding site on the regulatory light chain is a probable binding location, although other sites of calcium binding are possible, including non-specific binding. Relevant to this question, calcium binding to single-headed heavy meromyosin decreases its radius of gyration, probably by binding the regulatory light chain and changing the conformation where the motor domain is attached to the rod portion of myosin (Harris et al., 1999). The regulatory light chain abuts the myosin rod, and the calcium-induced decrease in the hydrodynamic size of S1, detected by TEB, is consistent with a conformational change in the regulatory light chain region. In any event, the effects of free and nucleotide-chelated calcium binding on S1 conformation appear to be independent (Table 1), and the free calcium binding was not pursued further.

The S1 · CaADP · V_i complex is stable, at least in the presence of a small excess of orthovanadate. The rates of formation and dissociation (Table 2) indicate that the calcium complex is less stable than the magnesium complex by two orders of magnitude. The dissociation rates in the presence of EDTA are similar. The difference in stability is due to differences in the rates of association, suggesting that a protein conformational change occurring after CaADP and V_i have bound is slower for the calcium complex. In the absence of EDTA the dissociation of V_i from S1 · MgADP · V_i has a half-time of days (Goodno, 1982), and the nucleotide is considered to be "trapped." Whether the nucleotide is actually trapped in S1 · CaADP · V_i was not investigated.

The actin-activation of CaATPase activity (Fig. 3) indicates that actin interacts with the steady-state intermediate. The inhibition of CaATPase activity at high [actin] strengthens the conclusion that the activation at low [actin] is due to actin binding to S1 · CaADP · P_i rather than to S1 · CaATP. This interaction in solution is consistent with myosin · CaATP · P_i binding to the thin filament to generate force in fibers, and satisfies requirement four above. The actin-activated S1 CaATPase activity is similar to that of MgATPase, but the activation is much smaller because the higher basal CaATPase activity (Table 3). The higher basal CaATPase activity indicates the rate of P_i dissociation in the absence of actin is increased. The reduced stability of S1 · CaADP · V_i compared to S1 · MgADP · V_i is consistent with this idea, although the kinetic data above suggest the difference in stability is due to a step on the pathway to forming S1 · CaADP · V_i, rather than its decomposition.

Requirement four in the list above is not demonstrated here for CaATP hydrolysis. There are data indicating lever arm rotation occurs while a motor domain is bound to actin (Whittaker et al., 1995; Uyeda et al., 1996; Gollub et al., 1996; Baker et al., 1998; Hopkins et al., 1998), but direct detection of lever arm motion during force production for any substrate remains elusive. The detailed nature of the reverse rotation is not known. Indeed, the term "reverse" is being used for convenience; the actin-free and actin-bound trajectories are probably different. Based on high-resolution structures of S1 and S1 · MgADP · AlF_4, the motion in the absence of actin may involve rotations about two fulcrum sites (Rayment et al., 1993; Dominguez et al., 1998). In muscle fibers that have fluorescent probes attached to the

lever arm, the motion appears to include rotation about the long axis of the lever arm and axial rotation about a fulcrum (Hopkins et al., 1998). The magnitude of force produced by CaATP (Fig. 1), 20% of that obtained with MgATP, is at least consistent with the two substrates supporting similar mechanisms for the actin-bound cross-bridge motion.

The fifth requirement is met. The actin interactions of S1 · CaADP and S1 · CaADP · P_i are similar to those of their magnesium counterparts. The increase in binding energy for the transition from A · S1 · CaADP · $P_i \rightarrow$ A · S1 · CaADP + P_i is somewhat larger than it is for the comparable transition when magnesium is present (Table 4), due the greater affinity of S1 · CaADP for actin. The change in apparent electric charge at the interface is comparable, whether the complexes contain calcium or magnesium.

Taken together, the data are fully consistent with the lever arm model of force production being applicable to force generation by CaATP hydrolysis. This answers the primary question being investigated here. Given the similarity of the calcium and magnesium data regarding lever arm rotation and actin interactions in solution, one can ask why the force produced by glycerinated muscle fibers in the presence of calcium is smaller. There are several possible explanations that are consistent with the above data, although this secondary question cannot be answered unequivocally at this time.

One possibility is that the reduced force is due to the higher affinity of a cross-bridge · CaADP complex for actin, which keeps the cross-bridge bound to actin longer, and creates an opposing force that is greater than the MgADP complex does during the fiber hydrolytic cycle. An increased opposing force, if real, would be expected to have a greater role when shortening is occurring than for isometric force, as measured in the present study. A second possibility is that the reduced force observed with CaATP may be due to the high basal CaATPase activity. The lifetime of the steady-state intermediate S1 · MgADP · P_i is 36-fold greater than that of S1 · CaADP · P_i, as estimated by the reciprocals of the steady-state activities in Table 3. It may be that in a fiber, myosin · CaADP · P_i is more likely than myosin · MgADP · P_i to dissociate P_i before it binds to actin. If hydrolysis and force production were uncoupled, more heat would be produced by fibers performing work by hydrolyzing CaATP. However, a third possibility is that force is reduced because the rate of hydrolysis is slower for CaATP that it is for MgATP, when a cross-bridge is bound to actin. The rate for MgATP drops by ~50% from the V_{max} value when the [actin] is high enough to saturate S1 · MgATP (White et al., 1998). We could not obtain a value for S1 · CaATPase activity at saturating [actin] (Fig. 4), but for isometric force conditions the fiber [actin] may reduce CaATPase activity to levels lower than MgATPase activity. Finally, it is possible that lever arm motion occurs when the motor domain is bound to actin, but it is "less forceful" when Ca^{2+} is bound. Ca^{2+} may distort the structure in the fulcrum region (see Dominguez et al., 1998), changing the trajectory taken and/or force produced. As discussed above, the details of the motion of a force-producing lever arm are not known. Analogous to the G-protein family members, myosin has a switch II located near the ATP site (Smith and Rayment, 1996b) which may be part of an allosteric pathway from the ATP site to the fulcrum region (Kirshenbaum et al., 1999). The TEB data (Table 1) suggest that there are only small, if any, differences in the degree of rotation of the lever arm when calcium replaces magnesium for free S1 · MgADP · V_i. However, near-ultraviolet circular dichroism measurements indicate that there are structural differences between S1-ADP-phosphate analog complexes made with calcium and magnesium (Peyser et al., 1997). Even small changes in the structure of the ATP site-switch II-fulcrum region could change the amount of force produced by the reverse rotation of the lever arm under a load.

We thank Roger Cooke for useful discussion of the results.

This work was supported by National Institutes of Health Grants AR42895 (to K.P. and S.H.), GM52588 and RR11805 (to D.E.), and HL32145 (to M.C.).

REFERENCES

Ajtai, K., D. Fang, S. Park, C. R. Zayas, Y. M. Peyser, A. Muhlrad, and T. P. Burghardt. 1998. Near UV circular dichroism from biomimetic model compounds define the coordination geometry of vanadate centers in MeVi-and MeADPVi-rabbit myosin subfragment 1 complexes in solution. *Biophys. Chem.* 71:205–220.

Baker, J. E., I. Brustmascher, S. Ramachandran, L. E. W. Laconte, and D. D. Thomas. 1998. A large and distinct rotation of the myosin light chain domain occurs upon muscle contraction. *Proc. Natl. Acad. Sci. U.S.A.* 95:2944–2949.

Bowen, W. J. 1952. Phosphorylysis of adenosine triphosphate and rate of contraction of myosin B threads. *Am. J. Physiol.* 165:10–14.

Cooke, R. 1997. Actomyosin interaction in striated muscle. *Physiol. Rev.* 77:671–697.

Cooke, R., and E. Pate. 1985. The effects of ADP and phosphate on the contraction of muscle fibers. *Biophys. J.* 48:789–798.

Dominguez, R., Y. Freyzon, K. M. Trybus, and C. Cohen. 1998. Crystal structure of a vertebrate smooth muscle myosin motor domain and its complex with the essential light chain: visualization of the pre-power stroke state. *Cell.* 94:559–571.

Eden, D., and S. Highsmith. 1997. Light chain-dependent myosin structural dynamics in solution investigated by transient electrical birefringence. *Biophys. J.* 73:952–958.

Elias, J. G., and D. Eden. 1981. Transient electric birefringence study of the persistence length and electrical polarizability of restriction fragments of DNA. *Macromolecules.* 14:410–419.

Geeves, M. A., and K. C. Holmes. 1999. Structural mechanism of muscle contraction. *Annu. Rev. Biochem.* 68:687–728.

Gollub, J., C. R. Cremo, and R. Cooke. 1996. ADP release produces a rotation of the neck of smooth myosin but not skeletal myosin. *Nat. Struct. Biol.* 3:796–802.

Goodno, C. C. 1979. Inhibition of myosin ATPase by vanadate ion. *Proc. Natl. Acad. Sci. U.S.A.* 76:2620–2624.

Goodno, C. C. 1982. Myosin active-site trapping with vanadate ion. *Methods Enzymol.* 85:116–123.

Harris, S. P., S. Gallagher, C. Warren, and M. L. Greaser. 1999. Ca^{2+}-induced structural rearrangements in skeletal muscle myosin subfragments as assessed by small angle x-ray scattering. *Biophys. J.* 76:50*a*. (Abstr.).

Highsmith, S. 1997. Myosin regulatory light chain and nucleotide modulation of actin binding site electric charge. *Biochemistry.* 36:2010–2016.

Highsmith, S. 1999. Lever arm model of force production by actin-myosin-ATP. *Biochemistry.* 38:9791–9797.

Highsmith, S., and D. Eden. 1990. Ligand-induced myosin subfragment 1 global conformational change. *Biochemistry.* 29:4087–4093.

Highsmith, S., and A. J. Murphy. 1992. Electrostatic changes at the actomyosin-subfragment 1 interface during force-generating reactions. *Biochemistry.* 31:385–389.

Hopkins, S. C., C. Sabido-David, J. E. T. Corrie, M. Irving, and Y. E. Goldman. 1998. Fluorescence polarization transients from rhodamine isomers on the myosin regulatory light chain in skeletal muscle fibers. *Biophys. J.* 74:3093–3110.

Kirshenbaum, K., M. Young, and S. Highsmith. 1999. Predicting allosteric switches in myosins. *Protein Sci.* 8:1806–1815.

Kodama, T., K. Fukui, and K. Kometani. 1986. The initial phosphate burst in ATP hydrolysis by myosin and subfragment-1 studied by a modified Malachite green method for determination of inorganic phosphate. *J. Biochem. (Tokyo).* 99:1465–1472.

Lymn, R. W., and E. W. Taylor. 1971. Mechanism of adenosine triphosphate hydrolysis by actomyosin. *Biochemistry.* 10:4617–4624.

Margossian, S. S., and S. Lowey. 1982. Preparation of myosin and its subfragments from rabbit skeletal muscle. *Methods Enzymol.* 85:55–71.

Nauss, K. M., S. Kitagawa, and J. Gergely. 1969. Pyrophosphate binding to and adenosine triphosphatase activity of myosin and its proteolytic fragments. *J. Biol. Chem.* 244:755–765.

Nihei, T., and Y. Tonomura. 1959. Kinetic Analysis of the myosin B-ATPase system. *J. Biochem. (Tokyo).* 46:305–319.

Pate, E., K. Franks-Skiba, H. White, and R. Cooke. 1993. The use of differing nucleotides to investigate cross-bridge kinetics. *J. Biol. Chem.* 268:10046–10053.

Peyser, Y. M., K. Ajtai, M. M. Werber, T. P. Burghardt, and A. Muhlrad. 1997. Effect of metal cations on the conformation of myosin subfragment-1-ADP-phosphate analog complexes: a near-UV circular dichroism study. *Biochemistry.* 36:5170–5178.

Peyser, Y. M., M. Benhur, M. M. Werber, and A. Muhlrad. 1996. Effect of divalent cations on the formation and stability of myosin subfragment 1-ADP-phosphate analog complexes. *Biochemistry.* 35:4409–4416.

Pitzer, K. S. 1979. Theory: ion interaction approach. *In* Activity Coefficients in Electrolyte Solutions. R. M. Pytkowitc, editor. CRC Press, Baton Rouge. 157–208.

Provencher, S. W. 1976. An eigenfunction expansion method for the analysis of exponential decay curves. *J. Chem. Phys.* 64:2772–2777.

Rayment, I., W. R. Rypniewski, K. Schmidt-Base, R. Smith, D. R. Tomchick, M. M. Benning, D. A. Winkelmann, G. Wesenberg, and H. M. Holden. 1993. 3-Dimensional structure of myosin subfragment-1—a molecular motor. *Science.* 261:50–58.

Shriver, J. W., and B. D. Sykes. 1981. Phosphorus-31 nuclear magnetic resonance evidence for two conformations of myosin subfragment-1 nucleotide complexes. *Biochemistry.* 20:2004–2012.

Smith, C. A., and I. Rayment. 1996a. X-ray structure of the Mg(II) · ADP · vanadate complex of the *Dictyostelium discoideum* myosin motor domain to 1.9 angstrom resolution. *Biochemistry.* 35:5404–5417.

Smith, C. A., and I. Rayment. 1996b. Active site comparisons highlight structural similarities between myosin and other P-loop proteins. *Biophys. J.* 70:1590–1602.

Spudich, J. A., and S. Watt. 1971. The regulation of rabbit skeletal muscle contraction. *J. Biol. Chem.* 246:4866–4871.

Szent-Gyorgyi, A. 1947. Chemistry of Muscular Contraction, 1st ed. Academic Press Inc., New York. 118–119.

Uyeda, T. Q. P., P. D. Abramson, and J. A. Spudich. 1996. The neck region of the myosin motor domain acts as a lever arm to generate movement. *Proc. Natl. Acad. Sci. U.S.A.* 93:4459–4464.

Wagner, P. D., and E. Giniger. 1981. Hydrolysis of ATP and reversible binding to F-actin by myosin heavy chains free of all light chains. *Nature.* 292:560–562.

Weber, H. H., and H. Portzehl. 1954. Transference of the muscle energy. *Prog. Biophys. Biophys. Chem.* 4:60–111.

Weeds, A. J., and R. S. Taylor. 1975. Separation of subfragment-1 isozymes from rabbit skeletal muscle myosin. *Nature.* 257:54–56.

White, H. D., B. Belknap, and M. R. Webb. 1997. Kinetics of nucleoside triphosphate cleavage and phosphate release steps by associated rabbit skeletal actomyosin measured using a novel fluorescent probe for phosphate. *Biochemistry.* 36:11828–11836.

White, H. D., and E. W. Taylor. 1976. Energetics and mechanism of actomyosin adenosine triphosphatase. *Biochemistry.* 15:5818–5826.

Whittaker, M., E. M. Wilson-Kubalek, J. E. Smith, L. Faust, R. A. Milligan, and H. L. Sweeny. 1995. A 35 Å-movement of smooth muscle myosin on ADP release. *Nature.* 378:748–751.